Homogeneous Binary Zirconocenium Catalyst Systems for Propylene Polymerization. 1. Isotactic/Atactic Interfacial Compatibilized Polymers Having Thermoplastic Elastomeric Properties[⊥]

James C. W. Chien,*,†,§,∥ Yasumasa Iwamoto,† Marvin D. Rausch,† Wolfgang Wedler,‡ and Henning H. Winter‡

Departments of Chemistry, Chemical Engineering, and Polymer Science and Engineering, University of Massachusetts, Amherst, Massachusetts 01003, and Amherst Polymer Technology, Inc., Amherst, Massachusetts 01002

Received November 25, 1996; Revised Manuscript Received March 17, 1997[⊗]

ABSTRACT: Polypropylene with thermoplastic elastomeric properties was synthesized by homopolymerization of propylene using two metallocene catalysts of different stereospecificities: *rac*-ethylenebis(1-η^5-indenyl)zirconium dichloride or *rac*-dimethylsilylenebis(1-η^5-indenyl)zirconium dichloride as isospecific catalyst precursors and ethylenebis(9-η^5-fluorenyl)zirconium dichloride as an aspecific precursor. The catalysts formed by activation of the precursors with triphenylcarbenium tetrakis(pentafluorophenyl)-borate and triisobutylaluminum exhibit a very high activity of 5×10^7 g of PP/([Zr][C_3H_6] h). Products ranging from tough plastomers to weak elastomers were obtained by varying the ratio of the two types of precursors. The polymers containing less than half of the isotactic fraction display excellent thermoplastic elastomeric properties, which is attributable to an interconnected crystalline superstructure in an amorphous continuum compatibilized and bound together by a stereoblock copolymer at the interface against macrophase separation. Materials exhibiting elastic recoveries of 97−98%, which are relatively independent of elongation up to 500%, were obtained.

Introduction

The first Ziegler−Natta coordination catalysts comprise active centers with different stereospecificities which produced polypropylenes of different stereoisomeric structures.[1,2] Most of the subsequent developments in heterogeneous Ziegler−Natta catalysts, especially those in the industrial laboratories, were directed mainly toward maximizing the high stereoselective sites, which produce the valuable isotactic polypropylene (*i*-PP), and diminishing the low stereoselective centers, which form the stereoregular polypropylenes, by selective poisoning.[3]

The synthesis of polypropylenes with lower levels of stereoregularity have received some belated attention. The objective is to produce polypropylenes with useful elastomeric properties. Early efforts,[4] including those of Natta et al.,[1,2] did not result in a practical process. Not only were catalyst productivities low but also only a portion of the product had the desired properties, requiring removal of the isotactic fractions in order to isotate the elastomeric polymer.

Collett et al.[5a] of the Du Pont Co. made heterogeneous catalysts by reacting transition-metal alkyls R_4M (R is $PhCH_2$, $(CH_3)_3C$, or $PhC(CH_3)_2C$; M is Zr, Ti, or Hf) with partially dehydroxylated Al_2O_3, which polymerize propylene to afford elastomeric PP (herein given as *el*-PP**A**). The inventors demonstrated that the key component resposible for the elasticity is a high molecular weight ether-soluble fraction that can cocrystallize with more stereoregular components to form a cross-linked network. It seems likely that these catalysts comprise centers possessing both high and low stereoselectivities.

Wilson and Job[6a] disclosed a high productivity catalyst formed by reacting magnesium ethoxide with $TiCl_4$ in the presence of veratrole (1,2-dimethoxybenzene). It produces polypropylene (herein given as *el*-PP**B**) which is predominantly isotactic (greater than 60%), but also contains about 20% syndiotactic sequences and 15−25% atactic units.[7]

Advance in metallocene chemistry[8] had led to the discoveries of many "single-site" catalysts. Metallocene precursors belonging to C_2, C_s, or C_{2v} space groups were shown to produce *i*-PP,[9,10] syndiotactic polypropylene (*s*-PP),[11,12] and atactic polypropylene (*a*-PP).[13,14] The C_{2v} systems are employed for the production of linear low density polyethylene and ethylene−cycloolefin copolymers having narrow molecular weight and comonomer composition distributions. Chien et al.[15] invented an asymmetric titanocene catalyst (**C**) to catalyze both stereospecific and stereorandom propylene insertion by the two interconverting sites i and **a**, respectively, as depicted in Scheme 1.[15,16] The elastic stereoblock polypropylene product (herein given as *el-sb*-PP**C**), has a well-defined alternating crystalline (isotactic) amorphous (atactic) block microstructure which possesses low hysteresis and high recovery elastic properties.[16] Essentially the same type of material (herein given as *el-sb*-PP**D**) was obtained with nonbridged zirconocenes having an indenyl ligand with a bulky substituent[17] (**D**), which can interconvert between a *rac*-like site to a *meso*-like site as proposed in Scheme 2. Catalysts **C** and **D** both have low to modest productivities and produce *el*-PP with desired properties only within a narrow window of polymerization conditions, i.e. temperature (T_p) and propylene pressure. Significant changes in polymer microstructure usually require a different metallocene.[17,18]

† Department of Chemistry, University of Massachusetts.
‡ Department of Chemical Engineering, University of Massachusetts.
§ Department of Polymer Science and Engineering, University of Massachusetts.
∥ Amherst Polymer Technology, Inc.
⊥ A preliminary report was given at the Symposium on Single-site Catalysis, 211th National Meeting of the American Chemical Society, New Orleans, LA, Mar 26, 1996.
⊗ Abstract published in *Advance ACS Abstracts,* May 15, 1997.

S0024-9297(96)01726-3 CCC: $14.00

Scheme 1

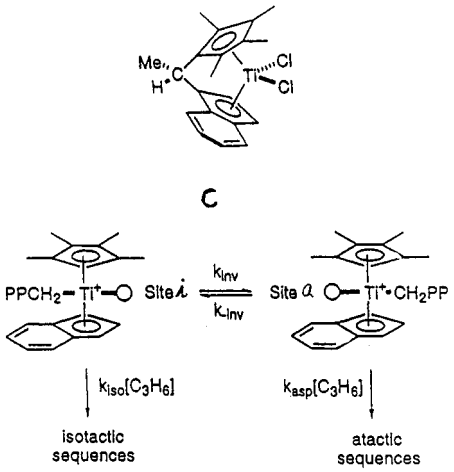

Scheme 2

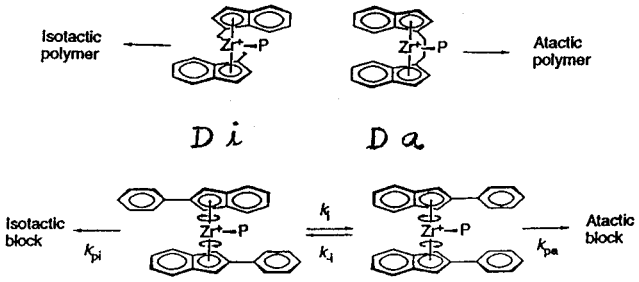

The central purpose of this research effort is to find novel ways to produce *el*-PP. We report here a new process using a C_2 and C_{2v} symmetric homogeneous binary catalyst (*HBC*) to produce polypropylenes wherein the percentages of *i*-PP and *a*-PP, their molecular weights, isotacticities, and melting transition temperatures (T_m) can all be independently controled and varied. Fractionation and NMR studies showed that the HBC process produces *sb*-PP in addition to the expected *i*-PP and *a*-PP. The physical, mechanical, and rheological properties of the present *el*-PP**E** are described and its elastic properties are compared with those of *el*-PP**A** to **D**. A possible mechanism explaining the formation of *sb*-PP by the *HBC* process is proposed.

Experimental Section

Materials. Solvents were dried over a Na/K alloy or CaH_2 and distilled under argon prior to use. Methylaluminoxane (MAO) was obtained from Akzo Chemicals. Polymerization grade propylene was purchased from Mariam Graves and purified by passing through two Matheson Gas Purifiers (Model 6404). Davison 952 silica was a gift from Grace. Unless otherwise indicated, all other chemicals were obtained from Aldrich.

Synthesis. All reactions were carried out using Schlenk or glovebox techniques under an argon atmosphere. Previously detailed procedures were used to synthesize *rac*-ethylenebis(1-η^5-indenyl)zirconium dichloride (**1**),[10b] *rac*-dimethylsilylenebis(1-η^5-indenyl)zirconium dichloride (**2**),[19] ethylenebis(9-fluorenyl)zirconium dichloride (**3**),[13,14] and triphenylcarbenium tetrakis(pentafluorophenyl)borate, $[Ph_3CB(C_6F_5)_4]$ (**4**).[10d] Routine ^{1}H NMR spectra were recorded on a Bruker NR-80 spectrometer at ambient temperature in $CDCl_3$; chemical shifts were referenced with respect to TMS.

Supported Catalyst. The silica-supported zirconocene catalyst was prepared by an earlier published procedure,[20] which was modified to impregnate two zirconocene precursors. Silica (Davison #952, 1 g) was heat-treated at 320 °C under a stream of argon for 20 h followed by heating at 200 °C for 10 h in vacuo. This partially dehydroxylated silica was dispersed in 10 mL of 0.6 M MAO solution in toluene. After overnight stirring at 50 °C, the MAO/SiO_2 material was filtered under argon, washed with toluene four times, mixed with 20 mL of toluene containing 0.02 mmol of **2** and 0.08 mmol of **3**, and stirred overnight at 50 °C. After filtration under Ar, the product was washed with toluene four times and dried under vacuum. This supported catalyst, **2**/**3**/MAO/SiO_2, has the following elemental analysis: Al, 9.0 wt %; Zr, 0.66 wt %. The former corresponds to 3.3 mmol of Al; hence, about half of the MAO added to silica reacted with the surface silanol groups for slightly less than the theoretical coverage.[21] The 0.072 mmol of Zr in the catalyst corresponds to about two-thirds of the combined **2** and **3** used in the preparation. This catalyst is referred to herein as the SD4 or supported binary catalyst.

A single zirconocene supported catalyst (SD3) was also prepared as above using only 0.02 mmol of **2**. The resulting catalyst **2**/MAO/SiO_2 was analyzed to contain 0.14 wt % of Zr. This represents 0.015 mmol of Zr and corresponds to about two-thirds of **2** employed in the preparation of SD3. Comparison of SD3 with SD4 suggests that **2** and **3** are immobilized in the latter case without a pronounced preference. It is likely that the zirconocenes are randomly and uniformly deposited. The polymerization results (vide infra) are consistent with this analysis.

Polymerization. Polymerization was carried out in a 250-mL crown-capped glass pressure reactor with a magnetic stirring bar. The system was first evacuated and flushed with argon, and then 50 mL of toluene was injected. The reactor was evacuated again and saturated with propylene for *ca*. 20 min to 15 psig. Triisobutylaluminum (TIBA) and then the zirconocenes were introduced as toluene solutions. The system was next equilibrated at the desired polymerization temperature (T_p). Finally, a quantity of the cocatalyst **4**, equal to all of the zirconocenes, was injected to initiate the polymerization. The order of addition of the reactants given above must be adhered to in order to achieve maximum catalytic activity. The polymerization mixture was quenched with acidic methanol (containing 2% HCl) and filtered off, and the resulting solid was washed with anhydrous methanol, and dried at about 70 °C under vacuum to constant weight.

Propylene Blends. The catalyst system **2**/**4**/TIBA was used to give *i*-PP; *a*-PP was obtained with the catalyst system **3**/**4**/TIBA. These polypropylene samples were combined to prepare blend specimens.

The solution-cast blend was prepared by codissolving *i*-PP and *a*-PP in the desired ratio under nitrogen atmosphere in one of three solvents: toluene (bp 110.6 °C), *p*-xylene (bp 137.8 °C), or mesitylene (bp 164.7 °C). The PP solution was poured into a Teflon dish, the solvent removed with a Dean Stark trap, and the solid dried under vacuum at 70 °C. About 1 wt % of BHT (2,6-di-*t*-butyl-4-methylphenol) was added as an antioxidant.

Quenched PP blend specimens were prepared by codissolving *i*-PP and *a*-PP in hot toluene under nitrogen atmosphere. This polymer solution was poured into an excess of methanol. The precipitated polymer was filtered and dried at 70 °C in vacuo.

Physical Characterization of Polymers. The polymer sample was fractionated with a Soxhlet apparatus to extract different stereoisomers of PP by refluxing acetone, diethyl ether, pentane, hexane, and heptane in a method devised by Pasquin.[22]

The T_g and heat of fusion (ΔH_f) were measured by differential scanning calorimetry (DSC; Perkin-Elmer DSC4). The sample was annealed at 180 °C for 10 min and crystallized by cooling at a rate of 10 °C/min to 50 °C in the instrument prior to recording of the DSC curve.

The crystalline structure of the prepared PP was determined by an X-ray diffractometer (XRD; Siemens D-500) using a Ni-filtered Cu Kα X-ray beam excited at 40 kV for $2\theta = 2-40°$ in 0.1° steps. The sample was either recorded as polymerized or as annealed at approximately 120 °C in vacuo for 1 h.

The microstructure of PP was determined on a ^{13}C NMR spectrometer (Bruker AMX-500; 125.77 MHz for ^{13}C) in C_2D_2-

Table 1. Propylene Polymerizations[a] Catalyzed by Single Catalyst System

run	precursor[b]	[Zr] (μM)	[**4**][c] (μM)	[TIBA] (mM)	T_p (°C)	time (min)	yield (g)	$A_p \times 10^{-7}$ (g of PP/(mol of Zr [C_3H_6] h))	T_m (°C)	ΔH_f (cal/g)
D147	**1**	10	10	5	0	15	2.15	1.9	149.5	17.2
D63	**2**	5	5	6	0	4	1.68	11.2	153.4	20.4
D77	**2**	20	20	5	50	20	8.64	8.3	130.6	14.8
D55	**3**	10	10	5	0	10	3.28	4.4		0
D152	**3**	10	10	5	25	20	3.88	5.4		0
D80	**3**	25	25	5	50	21	(4)	(3)		0

[a] $P_{C_3H_6}$ = 15 psig. [b] **1** = $Et(Ind)_2ZrCl_2$, **2** = $Me_2Si(Ind)_2ZrCl_2$, **3** = $Et(Flu)_2ZrCl_2$. [c] **4** = $Ph_3CB(C_6F_5)_4$.

$Cl_4/C_2H_2Cl_4$ mixed solvent at 110 °C. Chemical shifts were referenced with respect to TMS.

Mechanical and Elastic Measurements. The tensile stress behavior was studies with mechanical testing machines (Instron 5564 and 5811). A polypropylene flake was press-molded into a 15 mm long, 6 mm wide, and 0.7 mm thick dog-bone-shaped specimen at 175 °C. The specimen was subjected to strain imposed by an Instron machine at an uniaxial expansion rate of 150 mm/min (approximately 1000% gauge length/min).

The elastic property was characterized by two methods. In the first method, the specimen was elongated to 100, 200, 300, and 500% at an expansion rate of 150 mm with the Instron 5564 machine, stress was released immediately and quickly, and the recovery rate was obtained from the measured change in specimen length as a function of time.

The hysteresis curves of stress−strain behavior were measured on a mechanical testing machine (Instron 5564) by successively expanding and relaxing at 15 mm/min to approximately 100, 200, 300, 500, and 1000% and to the breaking point.

Rheological Studies. The flow properties of PP were investigated with a Rheometrics mechanical spectrometer (RMS-800). A standard procedure was employed for specimen preparation. PP was compression-molded under vacuum at about 180 °C into 25 mm diameter disk. This disk was inserted between the concentric-plate fixtures of the rheometer and heated to approximately 170 °C under a dry nitrogen atmosphere. A frequency−temperature cooling scan (FTCS) initiates a sequence of three tests for each material. The FTCS featured small oscillatory shear tests in a frequency range between 1 and 200 rad s^{-1}, with six discrete frequencies for each decade. The strain amplitudes chosen ranged between 0.08 and 0.01. Repeating the frequency measurement cycle after decreasing the temperature by 2 K steps afforded an average cooling rate of 0.7 K min^{-1} in the temperature interval between 80 and 180 °C. The response of the material yielded information about the dynamic shear moduli G' and G''. These quantities can be easily recalculated into loss angle, tan δ, and complex viscosity, η^*, data. Immediately after completing the FTCS, the frequency−temperature heating scan (FTHS) was initiated, beginning at the final temperature of the FTCS and using the same set of discrete frequencies and widths of the temperature steps. The FTHS was terminated after the specimen turned into the liquid state.

For the blended systems which showed phase transitions, a consecutive frequency scan (CFS) at a selected constant temperature was also performed to conclude the series of tests. After thermal equilibration at a temperature below the observed T_m of the crystallizing block, repeated frequency scans in intervals between 0.1 and 200 rad s^{-1} were carried out. The waiting time between the individual frequency scans ranged from 40 to 70 s.

Results and Discussion

Polymerization by a Single Zirconocenium Catalyst. Stereospecific polymerization of propylene to *i*-PP was catalyzed with either precursor **1** or **2**, while **3** was used in aspecific polymerization to obtain *a*-PP. Polymerization was performed at 0 °C using **4**/TIBA as the cocatalyst. The activity of polymerization for **1**/**4**/TIBA is 1.9×10^7 g of PP/(mol of Zr [C_3H_6] h), the *i*-PP product, designated as D147 has T_m = 149.5 °C and ΔH_f = 17.2 cal/g. Under the same conditions **2**/**4**/TIBA exhibited $A_p = 1.1 \times 10^8$ g of PP/(mol of Zr [C_3H_6] h). The *i*-PP obtained (D63) has T_m = 153.4 °C and ΔH_f = 20.4 cal/g (Table 1); the higher T_m and ΔH_f of D63 than D147 is consistent with the well-known superior stereoselectivity of precursor **2** than **1**.[10e] The non-selective **3**/**4**/TIBA polymerizes propylene with $A_p = 4 \times 10^7$ g of PP/(mol of Zr [C_3H_6] h) to give *a*-PP (D55).

Polymerization by Homogeneous Binary Zirconocenium Catalysts (HBC Systems). Propylene polymerizations were carried out with either the *HBC*-(**2**,**3**) or the *HBC*(**1**,**3**) catalyst in solution, where the numbers in the parentheses specify the precursors used. The reproducibility of polymerization was tested by running quadruplicates using the following conditions: [**2**] = 4 μM, [**3**] = 6 μM, [**4**] = 11 μM, [TIBA] = 6 mM, T_p = 0 °C, and $P_{C_3H_6}$ = 15 psig, in 20 mL of toluene. The polymer yields after 10 min of polymerization were 1.96, 2.22, 1.79, and 1.63 g, for an average of 1.90 ± 0.32 g. The A_p values were 4.4×10^7, 4.9×10^7, 4.0×10^7, and 3.6×10^7 g of PP/(mol of Zr [C_3H_6] h) for an average of $(4.23 \pm 0.55) \times 10^7$ g of PP/(mol of Zr [C_3H_6] h). The ±13% deviation in A_p is considered to be good reproducibility for Ziegler−Natta polymerizations under these conditions. The polypropylene produced has T_m values of 150.3, 150.9, 150.9, and 150.9 °C for an average of 150.7 ± 0.3 °C; the ΔH_f values were 2.4, 2.6, 2.9, and 2.5 cal/g for an average of 2.6 ± 0.2 cal/g.

Both *HBC* systems were used to polymerize propylene at ratios of **1** or **2** to **3** from 8:2 to 1:9 with several experimental conditions. The results are shown in Tables 2 and 3. The catalytic activities of these binary systems ($A_{p,o}$) listed in column 10 of both tables, lie in the range of $(1-10) \times 10^7$ g of PP/(mol of Zr [C_3H_6] h). These may be compared with expected $A_{p,c}$ calculated from single metallocene polymerization activities. In the case of **1**/**3**/**4**/TIBA, it is

$$A_{p,c} = m_{\mathbf{1}} A_{p,\mathbf{1}} + m_{\mathbf{3}} A_{p,\mathbf{3}} \qquad (1)$$

where $m_{\mathbf{1}}$ and $m_{\mathbf{3}}$ are the mole fractions of **1** and **3**, and $A_{p,\mathbf{1}}$ and $A_{p,\mathbf{3}}$ are their respective individual propylene polymerization activities. The $A_{p,o}$ values are in good agreement with the $A_{p,c}$ values. This is also the case for a similar comparison of the **2**/**3**/**4**/TIBA catalyst system.

The single metallocene **2** produces *i*-PP with ΔH_f = 20.4 cal/g. If this component forms the same *i*-PP in the presence of **3** in an *HBC* polymerization, then the expected $\Delta H_{f,c}$ of the product would be

$$\Delta H_{f,c}(\mathbf{2}/\mathbf{3}) = \frac{m_{\mathbf{2}} A_{p,\mathbf{2}}}{m_{\mathbf{2}} A_{p,\mathbf{2}} + m_{\mathbf{3}} A_{p,\mathbf{3}}} \times 20.4 \text{ cal/g} \qquad (2)$$

The expected $\Delta H_{f,c}$ of the product obtained with HBC(**1**,**3**) would be

Table 2. Propylene Polymerizations[a] Catalyzed by the *HBC*(2,3) System[b]

run no.	[**2**]:[**3**]	[**2**][b] (μM)	[**3**][b] (μM)	[**4**][b] (μM)	[TIBA] (mM)	T_p (°C)	time (min)	yield (g)	$A_p \times 10^{-7}$ (g of PP/(mol of Zr [C_3H_6] h)) obsd	$A_p \times 10^{-7}$ (g of PP/(mol of Zr [C_3H_6] h)) calcd[c]	T_m (°C)	ΔH_f (cal/g) obsd	ΔH_f (cal/g) calcd[d]	state[e]
D56	8:2	5	1.3	6.3	4	0	7	1.22	3.7	10.8	152.2	19.4	17.9	C
D58	5:5	4	4	8	4	0	6	1.52	4.2	8.9	152.2	16.3	13.6	L
D59	4:6	4	6	10	4	0	6	1.86	4.1	8.2	151.8	15.2	11.8	L
D60	3:7	3	7	10	4	0	10	0.70	1.0	7.6	151.2	5.4	9.2	F
D61	2:8	2	8	10	4	0	10	1.18	1.6	7.0	152.0	7.2	7.0	F
D62	1:9	1	9	10	4	0	10	0.95	1.3	6.3	151.0	3.1	3.8	F
D50	8:2	4	1	5	5	0	10	1.20	3.2	10.8	151.1	14.0	17.9	L
D51	6:4	5	3.3	8.3	5	0	10	3.10	5.0	9.5	149.8	15.7	15.3	L
D52	4:6	4	6	10	5	0	8	4.38	7.3	8.2	149.3	11.5	11.8	L
D53	2:8	2	8	10	5	0	8	3.24	5.4	7.0	150.0	8.9	7.0	F
D64	6:4	5	3.3	9.1	6	0	4	1.72	6.9	9.5	152.1	11.6	15.3	L
D65	5:5	4	4	8.8	6	0	4	1.55	6.5	8.9	151.8	9.0	13.6	L
D66	4:6	4	6	11	6	0	5	2.31	6.2	8.2	150.9	5.5	11.8	F
D67	3:7	3	7	11	6	0	5	2.63	7.0	7.6	150.7	3.9	9.2	E
D68	2:8	2	8	11	6	0	5	1.89	5.0	7.0	150.0	2.0	7.0	E
D79	2:8	5	20	25	5	50	20	4.39	3.4	4.0	123.9	6.5	5.9	E

[a] $P_{C_3H_6}$ = 15 psig. [b] **2** = $Me_2Si(Ind)_2ZrCl_2$, **3** = $Et(Flu)_2ZrCl_2$, **4** = $Ph_3CB(C_6F_5)_4$. [c] A_p(calcd) = $m_2A_{p,2} + m_3A_{p,3}$. [d] By eq 2. [e] C = crystalline; L = leathery; F = fluffy solid; E = elastomeric; G = gummy.

Table 3. Propylene Polymerizations[a] Catalyzed by the *HBC*(1,3) System[b]

run no.	[**1**]:[**3**]	[**1**][b] (μM)	[**3**][b] (μM)	[**4**][b] (μM)	[TIBA] (mM)	T_p (°C)	time (min)	yield (g)	$A_p \times 10^{-7}$ (g of PP/(mol Zr [C_3H_6] h)) obsd	$A_p \times 10^{-7}$ (g of PP/(mol Zr [C_3H_6] h)) calcd[c]	T_m (°C)	ΔH_f (cal/g) obsd	ΔH_f (cal/g) calcd[d]	state[e]
D158	8:2	8	2	10	5	0	12	1.91	2.1	2.8	147.7	7.4	9.8	E
D159	6:4	6	4	10	5	0	12	2.73	3.0	3.6	146.3	4.6	5.7	E
D160	4:6	4	6	10	5	0	12	2.47	2.7	4.4	146.0	2.2	3.1	E
D161	2:8	2	8	10	5	0	12	2.87	3.2	5.2	145.5	1.2	1.3	E
D162	1:9	1	9	10	5	0	30	1.60	0.7	5.6	145.3	0.5	0.6	E
D153	6:4	6	4	10	5	25	15	4.55	8.4		141.2	8.2		E
D154	4:6	4	6	10	5	25	15	4.33	8.0		140.5	5.7		E
D155	3:7	3	7	10	5	25	15	5.10	9.5		138.9	3.9		G
D156	2:8	2	8	10	5	25	15	5.34	9.9		137.9	2.7		G
D157	1:9	1	9	10	5	25	15	5.84	10.8		135.7	0.9		G

[a] $P_{C_3H_6}$ = 15 psig. [b] **1** = $Me_2Si(Ind)_2ZrCl_2$, **3** = $Et(Flu)_2ZrCl_2$, **4** = $Ph_3CB(C_6F_5)_4$. [c] A_p(calcd) = $m_2A_{p,2}+m_3A_{p,3}$. [d] By eq 1. [e] C = crystalline; L = leathery; F = fluffy solid; E = elastomeric; G = gummy.

$$\Delta H_{f,c}(\mathbf{1/3}) = \frac{m_{\mathbf{1}}A_{p,\mathbf{1}}}{m_{\mathbf{1}}A_{p,\mathbf{1}} + m_{\mathbf{3}}A_{p,\mathbf{3}}} \times 17.2 \text{ cal/g} \qquad (3)$$

However, the observed $\Delta H_{f,o}$ values are usually in discord with $\Delta H_{f,c}$; the variance appears to be influenced by the amount of TIBA present in the polymerization. For instance the PP's in Table II produced with small amounts of TIBA (4 mM) are slightly more crystalline than that expected for [**2**] $\gg$ [**3**] runs, where the deviation became negligible at [**2**] $\ll$ [**3**]. In the presence of high [TIBA] (6 mM), the rate of polymerization is enhanced and the polypropylene formed is highly elastic (vide infra). The products have much lower crystallinities than expected for [**2**] $\gg$ [**3**]; the crystallinity became greater at [**2**] $\ll$ [**3**]. Similar behaviors were manifested for catalysis by *HBC*(**1**,**3**) (Table 3).

The physical state of the *HBC*-PP undergoes systematic change as its $\Delta H_{f,o}$ deviates from the enthalpy of fusion expected by eq 2 or eq 3: $\Delta\Delta H_f = \Delta H_{f,c} - \Delta H_{f,o}$. When $\Delta\Delta H_f \leq 0$, the material resembles *i*-PP. As $\Delta\Delta H_f$ increases, the material assumes a leathery state and then becomes an elastomeric material. Finally, for *HBC* comprising an excess of C_{2v} metallocene **3**, a gummy product was formed, which is predominently amorphous PP.

The molecular weight distribution of PP formed by *HBC* is always broader than the most probable distribution. For instance the GPC chromatography of the polymer D-61 obtained with the *HBC*(**2**,**3**) system in a ratio of 2:8 has $M_n = 1.59 \times 10^5$, $M_w = 4.49 \times 10^5$, and $M_w/M_n = 2.82$.

Supported Metallocene Catalyst. Propylene was polymerized in the presence of a supported metallocene catalyst. SD3 is a catalyst of **2** supported alone on silica. At 0 °C using SD3 containing 60 μmol of Zr, activated with equal amount of **4** and 5 mM TIBA in 20 mL of toluene, propylene polymerized at an A_p of 5×10^4 g of PP/(mol of Zr [C_3H_6] h). The product has T_m = 153.9 °C and ΔH_f = 17.3 cal/g. The activity of silica-supported metallocene is generally an order of magnitude lower than that of the homogeneous catalysis,[20] but the cause is as yet uncertain. For instance, some zirconocene (precursor or cation) may reside in pores of silica which are too small or are overloaded with catalyst for the monomer to have easy access to the active center. There may also be side reactions between zirconocene species and the Brønsted acidic hydroxyls[23,24] or the Lewis basic oxide groups[25] to diminish the activity or even to alter the direction of stereoselection. For instance C_2 symmetric *ansa*-zirconocene supported on SiO_2 can have greatly enhanced stereospecificity.[26c] In the case of C_s symmetric *ansa*-zirconocene, its normally syndiospecific catalysis was changed to isospecific upon immobilization on silica.[27]

SD4 is a silica-supported catalyst prepared with **2**/**3** precursors in a ratio of 2:8. Its A_p value in toluene at 0 °C was 1.8×10^5 g of PP/(mol of Zr [C_3H_6] h). The PP produced has T_m = 149.1 °C and ΔH_f = 1.6 cal/g. The

Table 4. Thermal Properties of *i*-PP/*a*-PP Blends

blend component		sample			ΔH_f (cal/g)	
i-PP[a]	*a*-PP[b]	preparation	$T_{m,1}$ (°C)	$T_{m,2}$ (°C)	obsd	calcd[c]
1	1	ppt/MeOH	148.2[d]	145.7	11.7	10
1	1	evap/tol	147.5	145[d]	11.1	10
1	1	evap/xyl	145.1	140.3	9.5	10
1	1	evap/mes	145.1	139.8	8.7	10
3	7	evap/mes	147.6	138.0	7.1	6
1	9	evap/mes	148.0		1.8	2

[a] D-41. [b] D-55. [c] Calculated from (wt fraction *i*-PP) × 20.4. [d] Shoulder.

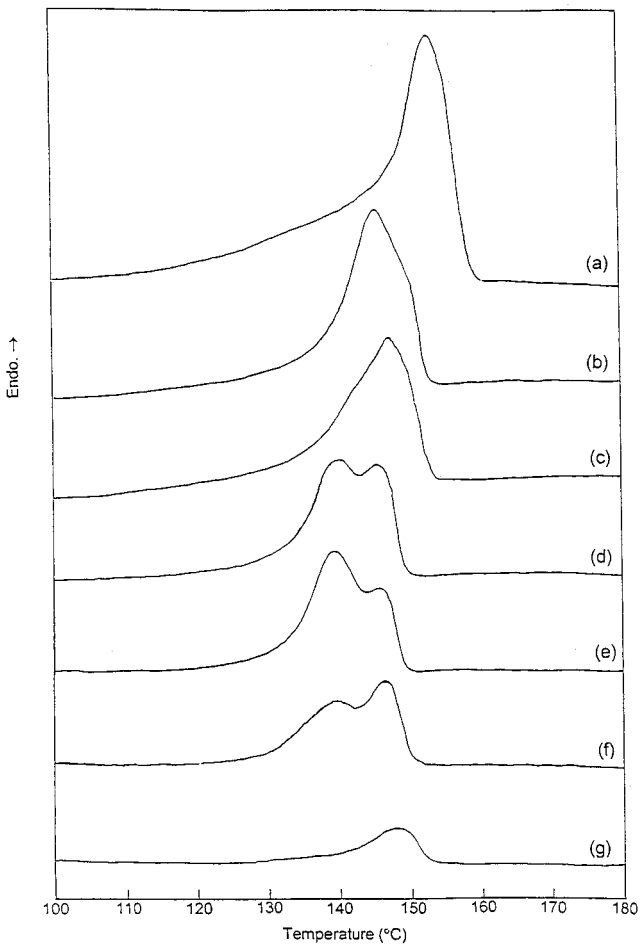

Figure 1. DSC melting thermograms: (a) *i*-PP; (b) mix 5 precipitated by methanol, *i*-PP:*a*-PP = 1:1; (c) mix 7 cast from toluene solution, *i*-PP:*a*-PP = 1:1; (d) mix 8 cast from *p*-xylene solution, *i*-PP:*a*-PP = 1:1; (e) mix 9 cast from mesitylene solution, *i*-PP:*a*-PP = 1:1; (f) mix 10 cast from mesitylene solution, *i*-PP:*a*-PP = 3:7; (g) mix 11 cast from mesitylene solution *i*-PP:*a*-PP = 1:9.

catalytic activity is markedly raised at $T_p = 25$ °C to $A_p = 7.9 \times 10^5$ g of PP/(mol of Zr [C_3H_6] h); the polypropylene produced has $T_m = 147.6$ °C and a higher ΔH_f of 2.8 cal/g.

Polymer Blends. The thermal properties of *i*-PP/*a*-PP blends are reported in Table 4. The DSC thermograms are shown in Figure 1. The blend samples have ΔH_f values close to the values calculated by

$$\text{wt fraction of } i\text{-PP} \times \Delta H_{f,i\text{PP}} \qquad (4)$$

using 20.4 cal/g for ΔH_f of the *i*-PP of this system. The agreement is indicative of macrophase separation into large crystalline domains. However, the T_m values of the blends are generally lower than that of the *i*-PP D41,

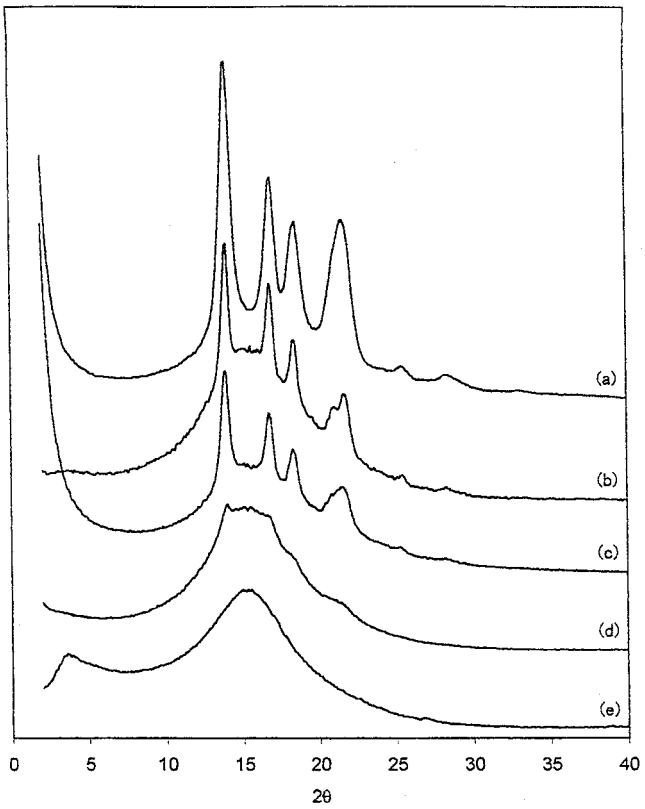

Figure 2. X-ray diffraction patterns: (a) *i*-PP (D53 **2**/**4**/TIBA, $T_p = 0$ °C, $\Delta H_f = 20.4$ cal/g); (b) mesitylene solution-cast blend (mix 10; *i*-PP:*a*-PP = 3:7, $\Delta H_f = 7.1$ cal/g); (c) supported binary catalyst (D_T105, [**2**]:[**3**] = 2:8, MAO/Zr = 3000/1, $T_p = 25$ °C, $\Delta H_f = 9.0$ cal/g); (d) *HBC* in solution (D66, [**2**]:[**3**] = 4:6, $T_p = 0$ °C, $\Delta H_f = 5.5$ cal/g); (e) *a*-PP (D55, **3**/**4**/TIBA, $T_p = 0$ °C).

and some of the thermograms even display two T_m peaks, which suggests the presence of smaller phase domains. The methanol-quenched blend exhibits the highest T_m among the blend specimens, which is interpreted to mean the absence of appreciable phase boundary mixing. The solution-cast blends have a lower T_m, a value which decreases as boiling point of the solvent increases. This suggests more mixing at phase boundaries and small crystallite sizes for specimens cast at high temperature.

Mesitylene solution-cast blend specimens were prepared with *i*-PP:*a*-PP ratios of 5:5, 3:7, and 1:9 designated as mix 9, mix 10, and mix 11, respectively. The first two materials exhibit two melting peaks; the lower T_m is found in the vicinity of 139 °C. This transition is too weak in mix 11 to be discerned. The upper transition increases in temperature as the *a*-PP content increases. However, the magnitude of ΔH_f changes in the opposite direction. On the basis of the values of T_m and ΔH_f, mesitylene solution-cast blends are judged to be better mixed than the other blends in Table 4.

X-ray Diffraction Analysis. The XRD patterns of various PP samples were compared in Figure 2. Pure *i*-PP is characterized by sharp α-type crystal reflections (Figure 2a), whereas only a diffuse amorphous halo is seen with *a*-PP (Figure 2e). The blend in Figure 2b has an XRD pattern which is a superposition of the two patterns indicating the presence of of *i*-PP domains. The *i*-PP reflections are considerably weaker and broader in the PP synthesized by a supported binary catalyst, which suggests smaller *i*-PP domains than in the former.

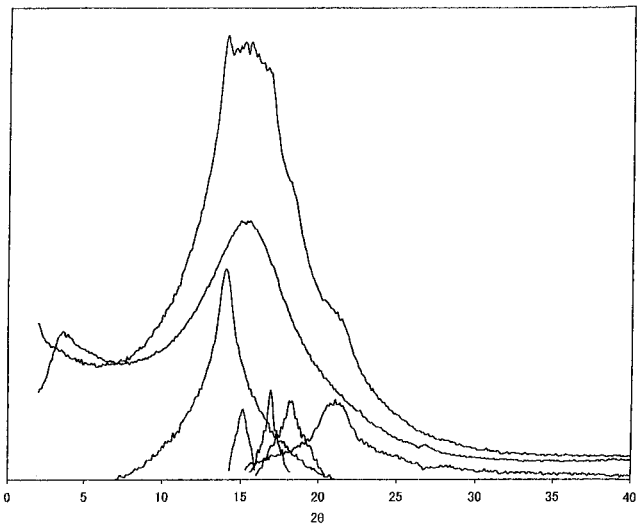

Figure 3. Deconvoluted XRD for D66 of Figure 2d.

The XRD of *HBC*-PP D-66 (Figure 2d) did not exhibit sharp reflections but only inflections at the appropriate 2θ positions superimposed on the background halo. Deconvolution analysis (Figure 3) showed the presence of α-type crystallites of the appropriate crystallinity. The expected heat of fusion was found by DSC determination. The broadness of these XRD reflections indicates the crystallites to be of minute dimensions.

Dynamic Viscoelastic Properties. Polymeric network formation can be treated rheologically as a gelation process.[16b] The formation of a gel is characterized by the emergence of a critical gel which presents an incipient transition state between a viscoelastic liquid (pregel) and a viscoelastic solid (postgel). The time dependence of its relaxation modulus ($G_c(t)$) features mathematical simplicity and is consistent with experimental observations.[28]

In this study, the solidification of the thermoplastic elastomeric polypropylenes (TPE-PP) sample was investigated using rheology to determine transition temperatures and rates for a wide range of blends with different composition in atactic and isotactic components. The variation of G^* vs temperature is given in Figure 4. A steplike function of large magnitude characterizes the melting and crystallization of the isotactic component. At the initially high temperatures the materials are viscoelastic liquids characterized by loss moduli mostly greater than storage moduli ($G'' > G'$). This information can be gained from additional plots of G', G'' vs frequency (same data in a different representation). The material is thermorheologically simple at these high temperatures: master curve construction and time−temperature superposition apply in the accessible frequency range without indication of morphological change. This analysis will be described elsewhere. At temperatures below T_m, the materials acquire properties of viscoelastic solids; the storage moduli are mostly greater than the flow moduli. Since crystallization progresses with a finite rate which is slower than the cooling rate, materials are not always in equilibrium during the cooling procedure. This can be seen from the differences between cooling and heating scans (compare parts a and b of Figure 4).

D61 PP obtained with *HBC* has initially the consistency of an heavily cross-linked rubber material with a high elastic modulus. The sample undergoes a phase transition, after which it shows the typical features of a fast relaxing, flowing, and viscoelastic liquid. It

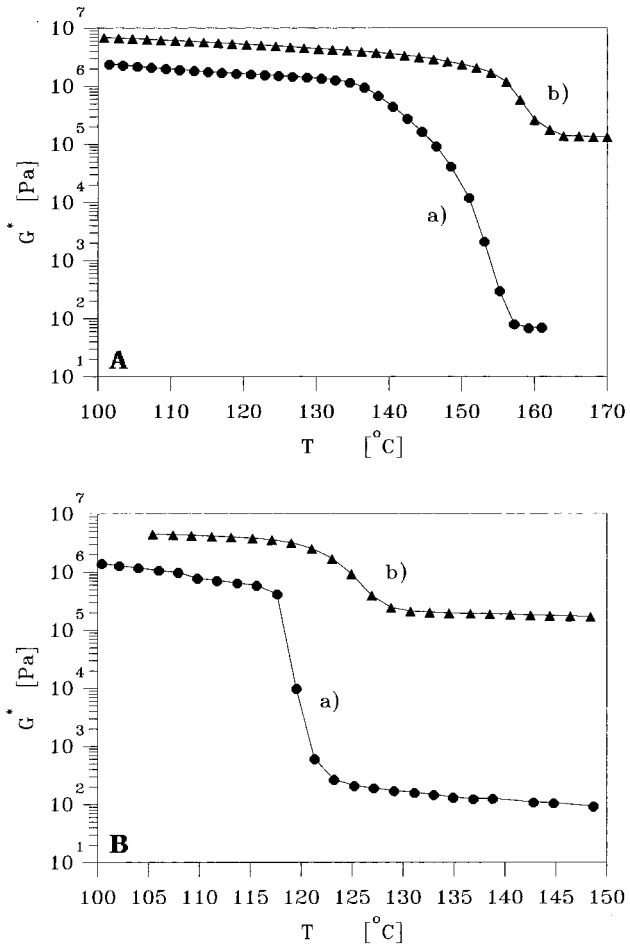

Figure 4. Complex modulus vs temperature comparison of (a) blend mixture 10, 35 wt % *i*-PP shown in O; (b) PP D61 made by binary catalyst **2**/**3** in 2:8 ratio containing *ca* 41 wt % of *i*-PP shown in Δ. Key: (A) heating scans at a constant frequency of 10 rad s^{-1}; (B) cooling scans.

behaves in the liquid phase like a compatible blend with a zero shear viscosity close to that of the pure *a*-PP. Blend mix 10 has almost the same composition and consists of components with the same molar weight as the *HBC* produced D61 and has a complex modulus below those of the pure constituents. The zero-shear viscosity at the same reference temperature is lower (by 2−3 orders of magnitude) than those of the pure components. This substantially contributes to the observed larger height of the step, and is a behavior which is characteristic for incompatible blends (depression of steady-shear viscosity by 0.5−1 order of magnitude) in the liquid phase. The very large change of G^* at the transition is then attributed to incompatibility of the broad components resulting in macrophase separation. In contrast D61, during crystallization, forms a co-continuous crystalline phase (to be envisioned e.g. as branched dendrites), penetrating the whole sample volume. This superstructure adds to the elasticity. The macrophase-separating blend, on the other hand, shows probably only spherulitic growth in the atactic matrix. The less branched superstructure yields less strength and lower moduli under same conditions of observation.

The PP obtained with a *HBC* such as **2**/**3** should produce, at 0 °C, *i*-PP and *a*-PP by the corresponding zirconocene species of 2×10^5 and 5×10^5 molecular weight, respectively, in amounts proportional to a 2:3 ratio. Figure 5 contains the G^* vs T data for five such polymers; their ΔH_f values are given in brackets. The

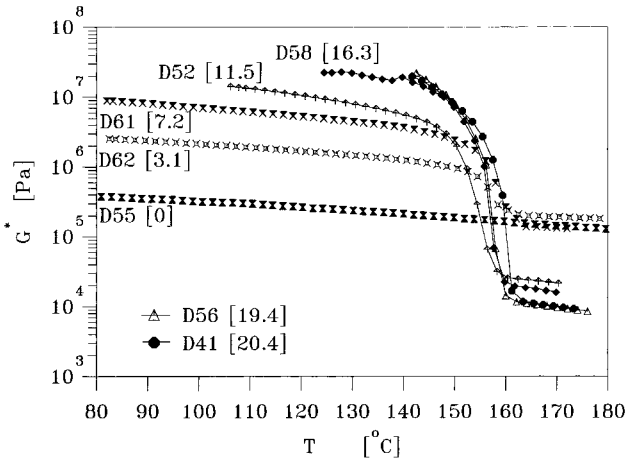

Figure 5. G^* vs T in five samples synthesized with *HBC*(**2**,**3**) at 0 °C and by **2** alone (D41) and **3** alone (D55) measured at 10 rad s^{-1}. Numbers in brackets give ΔH_f in cal g^{-1}.

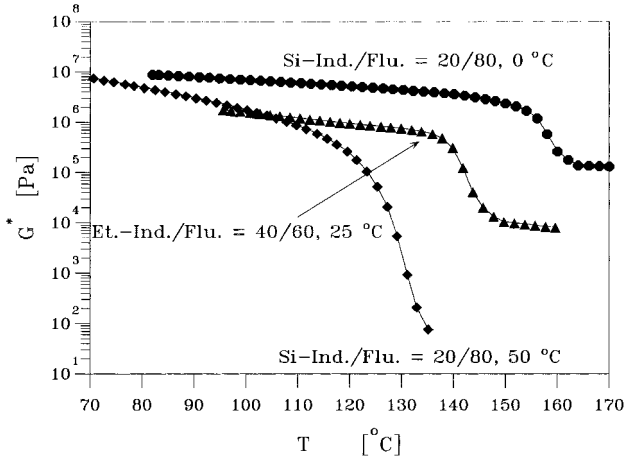

Figure 6. G^* vs T in sample synthesized by the catalyst and temperature as indicated at 10 rad s^{-1}.

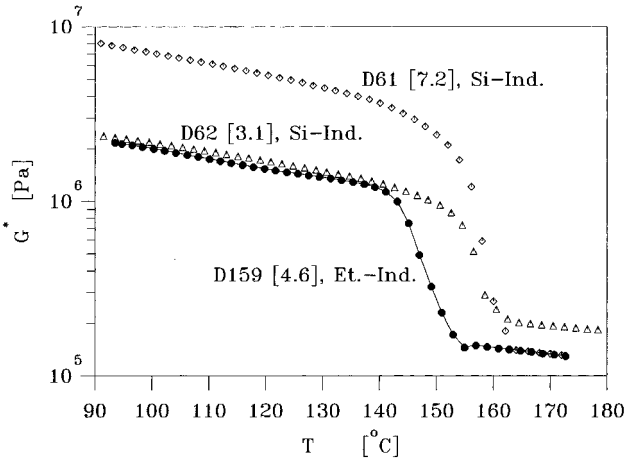

Figure 7. G^* vs T in samples synthesized by *HBC*(**2**,**3**) (D159) and by *HBC*(**1**,**3**) (D61) and (D62) at 0 °C.

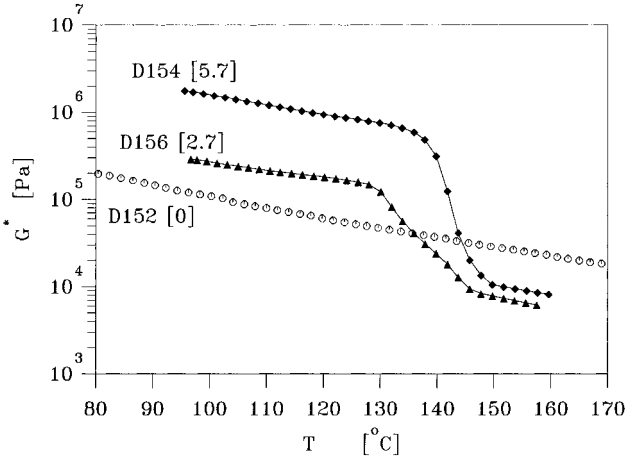

Figure 8. Same as Figure 7 except for polymerization at 25 °C.

results indicate a constancy of the phase transition temperatures but a strong dependence of the modulus changes on the composition. There is a direct correlation between phase transition enthalpy and the height of the ΔG^* step. The results suggest that an increasing amount of isotactic component leads to the formation of bigger, better developed, and interconnected crystalline domains, which increases the elasticity in the viscoelastic solid.

The versatility of the present synthesis of TPE–PP is the free choice of C_2 and C_{2v} symmetric precursors and the ratio of their concentrations (*vide supra*), T_p and monomer pressure. Figure 6 gives the data for PP formed by the *HBC*(**1**,**3**) and *HBC*(**2**,**3**) catalyst systems at three T_p values. The phase transition temperature and ΔG^* are strongly dependent on both T_p and on the C_2 symmetric precursor. To understand the contribution from the two factors, polymerizations were performed with the two catalyst systems at the same T_p (Figure 7). It is clear that catalyst **2**/**3** gave a lower phase transition temperature and G^* than **1**/**3**. Comparison of the behaviors of D154 and D156 in Figure 8, which were prepared at 25 °C with the D159 in Figure 7, showed the importance of T_p. A lower T_p gave an *HBC* PP with a higher transition temperature.

It is well-established that the molecular weight of PP catalyzed by **1** or **2** diminishes with the increase of T_p,[10] whereas a similar dependency is absent for **3**[14] for T_p < 70 °C. To show the influence of an increasing concentration of the low MW isotactic component on the relaxation time spectrum in the liquid phase, the G' and G'' data are plotted vs ω in Figure 9. Compared with the atactic components at the terminal zones, there is a steady shift of the curves toward higher frequencies with an increased content of *i*-PP for a similar molecular polydispersity at the same reference temperature. It indicates a steady shortening of the maximum relaxation time, caused by a decrease of average molecular weight. Figure 9a reveals further the difference between the *HBC*-PP D61 synthesized by the binary **2**/**3** catalyst in a 2:8 ratio and a solution-cast blend ("mixture 10") of the same composition with components synthesized at the same temperature as D61. The cast blend mixture has a much lower maximum relaxation time, resulting in a significantly lower viscosity. It behaves like a phase-separated or filled material probably because of the lower degree of interpretation of atactic and isotactic components than that seen in the *HBC* PP.

Mechanical Testing. Typical stress–strain curves obtained from expansion testing on selected materials (synthesized at 0 °C and molded at 175 °C) are given in Figure 10a. The *HBC*-PP (curve a) increases in strength with strain up to 1100% elongation which is characteristic of a cross-linked elastomer. The *a*-PP (curve d) does not show any yield point, but a nearly perfect stress plateau until break is considered to be due to the high degree of entanglement in the high molecular weight atactic polymer. The application of the high extension

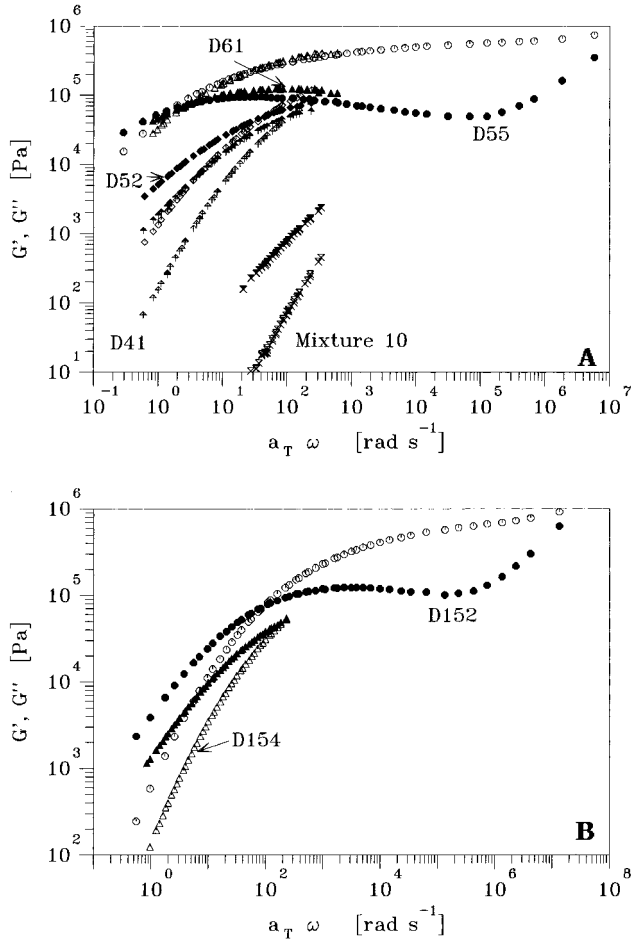

Figure 9. Influence of composition on relaxation time spectra in the liquid phase master curves for blends and PP synthesized at (A) $T_p = 0$ °C and (B) $T_p = 25$ °C.

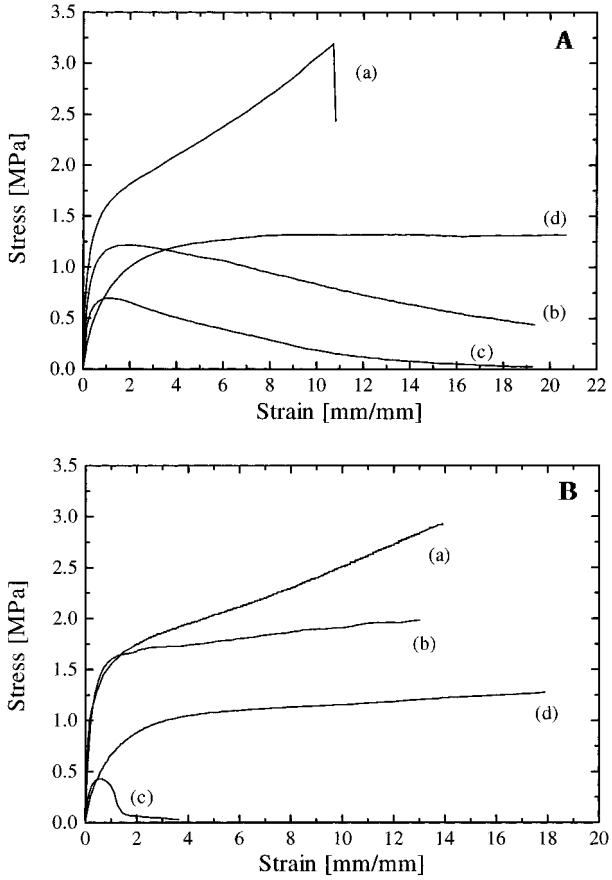

Figure 10. Influence of composition on mechanical strength, tested at room temperature with an expansion rate of 1000% gauge length per minute: molded at 175 °C (A); molded at 80 °C (B). Key: (a) HBC-PP D62; (b) SBC-PP D109; (c) PP blend mix 11; (d) *a*-PP (D55).

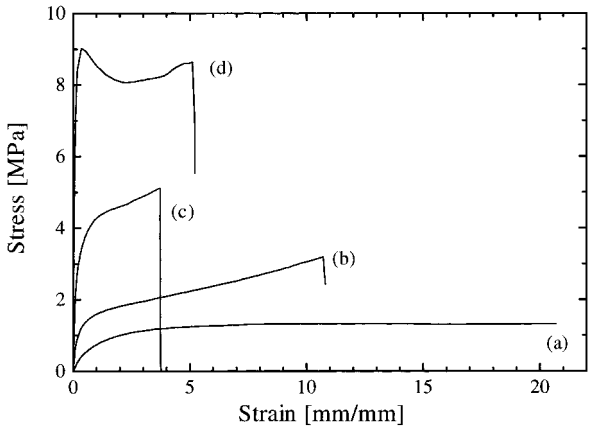

Figure 11. Stress−strain curves of (a) *a*-PP (D55) and HBC-PP synthesized with *HBC*(**2**,**3**) in a **2**:**3** ratio of (b) 1:9, D62, $\Delta H_f = 3.1$ cal/g; (c) 2:8, D61, $\Delta H_f = 7.2$ cal/g; and (d) 4:6, D52, $\Delta H_f = 11.5$ cal/g.

rate of 1000%/min does not allow the material to disentangle in experimental time and to flow. The PP produced by supported binary catalyst SD-4 has decreasing stress with strain after reaching the yield point (curve b). This is consistent with macrophase-separated domains. In the case of the PP blend, (mix 11, curve c) the decrease of strength is greater than in the former. This difference suggests fairly complete phase separation in the blend but some phase boundary mixing for the PP made with supported catalyst.

The mechanical property is of course sensitive to the sample preparation condition. To show the influence of the molding conditions, dog-bone specimens were also press molded at 80 °C; the data from the measurements are given in Figure 10b. Comparison with the results in Figure 10a showed virtually no difference in mechanical behavior for the *a*-PP molded at different temperatures. On the other hand the PP blend becomes a brittle substance without strength, indicating complete macrophase separation in this specimen. The *HBC*-PP is slightly weaker but has greater elongation to break in Figure 10b than in Figure 10a. This is consistent with growth of crystals to form stronger cross-links due to annealing effect in the latter. The opposite effect was observed for the PP obtained with supported binary catalyst, suggesting some phase mixing when molded at low temperature. Annealing at higher temperature promoted phase separation for this material.

The mechanical strength is dependent on the crystallinity of the *HBC*-PP. Figure 11 shows that an increasing content of *i*-PP increases Young's modulus. Simultaneously, the elongation to break drops from nearly 2000% to about 400%. With the exception of D52, which is too tough and slips at the grip, none of the other materials shows a yield point. If the different materials are compared, the observed stress plateau kept increasing with the content of isotactic component at high concentrations of *i*-PP, with a steady increase of stress until material failure was detected. The high moduli and plateau stresses of the three *HBC* polymers are regarded as due to the cross-linking effect of the interpenetrating crystalline structure of the *i*-PP. The observed increasing tendency in stress becomes stronger

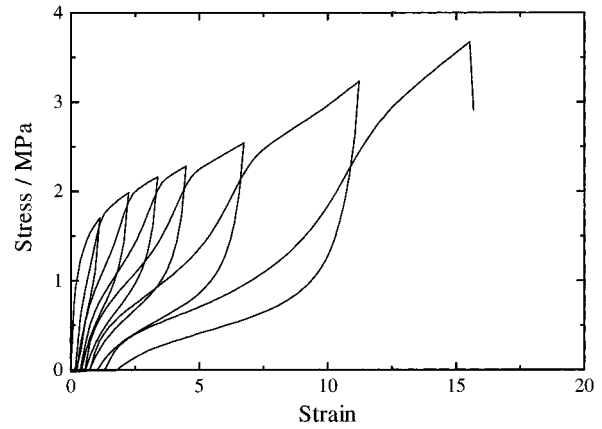

Figure 12. Relaxation testing at room temperature for PP D62 obtained with *HBC*(**2**,**3**) at a 1:9 ratio and 0 °C.

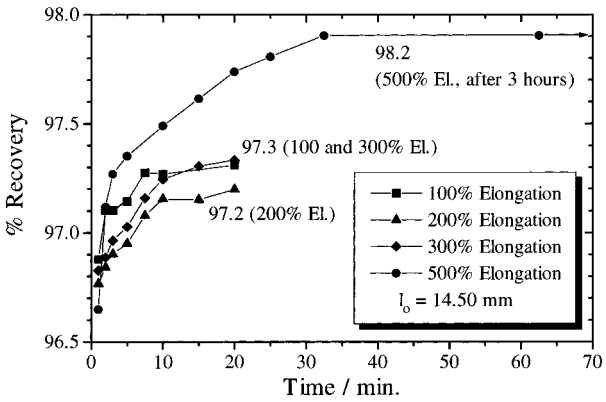

Figure 13. Percentage of elastic recovery for PP D62.

with the isotactic content, indicating stress-induced crystallization.

The comparison of D109 with a solution-cast blend (mix 11) further points to the influence that the degree of interpenetration has on elasticity. Polymer D109, synthesized with a supported catalyst, shows a high Young's modulus but low stress plateau at large strains. The failure occurs at a lower strain than for the *HBC*-PP of the same composition (D136). Perhaps the supported catalyst with its immobilized active centers produced a more segregated structure, with undisturbed and folded isotactic chains excluding the atactic component. As a result, the material behaves similar to a filled structure. This filler effect expresses itself even more strikingly when comparing it with the solution-cast blend. Mix 11 definitely has a higher Young's modulus than the *HBC*-PP of comparable composition, but fails already at strains of approximately 100%. Mechanical testing therefore shows that an interpenetrating crystalline structure in an amorphous matrix, as produced by *HBC*, has a positive effect on material elasticity and yields tough thermoplastic elastomers.

Elasticity. The *HBC*-PP displays outstanding elasticity. This is shown by the hysteresis curves of tensile stress measurements in Figure 12. The expansion curves returns to the previous stress at previous maximum strain. Figure 13 shows the percentage of recovery observed for the TPE-PP produced by *HBC* which was calculated by

$$\% \text{ recovery} = \frac{L_{max} - L_1}{L_{max} - L_0} \times 100\ (\%) \qquad (5)$$

where L_0, L_1 and L_{max} are the specimen lengths before elongation, after relaxation, and at maximum elongation, respectively. Although the residual expansion of the specimen were increased at higher strain, the recovery rate of the polymer was consistent at 97−98% between 100% to 500% elongation. In comparison, *a*-PP alone or a blend of *a*-PP with *i*-PP is virtually without elasticity according to these measurements.

Table 5. Hexane-Fractionation Results of Isotactic/Atactic Polymer

		C_6-soluble fraction		C_6-insoluble fraction		
polymer (run no.)	ΔH_f (cal/g)	wt %	% [*mmmm*]	wt %	% [*mmmm*]	% all other pentads
i-PP (D147)	20.4	5.9	<2	94.1	98	0
HBC-PP (D76)	2.3	89.8	2.4	10.2	44.1	55.9
SBC[a]-PP (D104)	4.5	74.7	3.0	25.3	98	<2
a-PP (D55)	0	100	<2			

[a] Supported binary zirconocene catalyst SD4.

Fractionation and ^{13}C-NMR Spectra. If the two zirconocenium species act completely independently of each other, then *HBC*-PP should be the same as *i*-PP/*a*-PP blend. Yet all the properties compared are very different, which may be explained by the formation of a material capable of compatibilizing *i*-PP and *a*-PP in *HBC*-PP.

Solvent extraction is the established method to separate a heterogeneous polymer specimen into components differing in microstructures.[22] Table 5 contains the hexane fractionation results. The *i*-PP (D147) obtained with the **2**/**4**/TIBA single zirconocene system comprises 5.9% hexane-soluble and 94.1% hexane-insoluble materials. The methyl region of the ^{13}C NMR spectrum for the hexane-insoluble fraction exhibits only the *mmmm* pentad resonance. The *a*-PP sample (D55) is completely soluble in hexane and shows the ^{13}C NMR spectrum expected for it. The D104 PP sample produced by the supported binary catalyst system is comprised of only hexane-insoluble *i*-PP and hexane-soluble *a*-PP, their relative amounts depending on the ratio of the two zirconocenes and on the polymerization condition.

Fractionation of D76, which is produced in the presence of **2**/**3** in 2:8 ratio activated with **4**/TIBA, afforded *ca*. 90% hexane-soluble and 10% hexane-insoluble polymers. The ^{13}C NMR spectra of the former (Figure 14b) is the same as that of *a*-PP (Figure 14a). However, the latter fraction's spectrum is a superposition of isotactic and atactic spectra (Figure 14c) in a 1:1.3 ratio. Therefore, D76 contains up to 10% of stereoblock copolymer.

To get a closer estimate of the content of stereoblock copolymer in a typical *HBC*-PP preparation (D52), it was fractionated using several solvents. Table 6 showed that about half of the D52 was soluble in diethyl ether, which has a ^{13}C NMR spectrum (Figure 15c) for *a*-PP. There is no material extractable by either pentane or hexane. The heptane-insoluble fraction showed a sharp *mmmm* resonance with some peaks for the other pentads (Figure 15a). The integrated intensity of the latter is about 11% of the total intensity. If one-fourth of the intensity in the *m* region is attributed to the atactic sequences and is subtracted from the total spectrum, then a content of approximately 6.5% *stereoblock PP* (sb-PP) can be estimated in this heptane-insoluble fraction. Finally, the ^{13}C NMR spectra of the heptane-soluble but hexane-insoluble fraction (Figure 15b) exhibits both a sharp *mmmm* peak and atactic peaks, which corresponds to *mm*, *mr*, and *rr* triads for

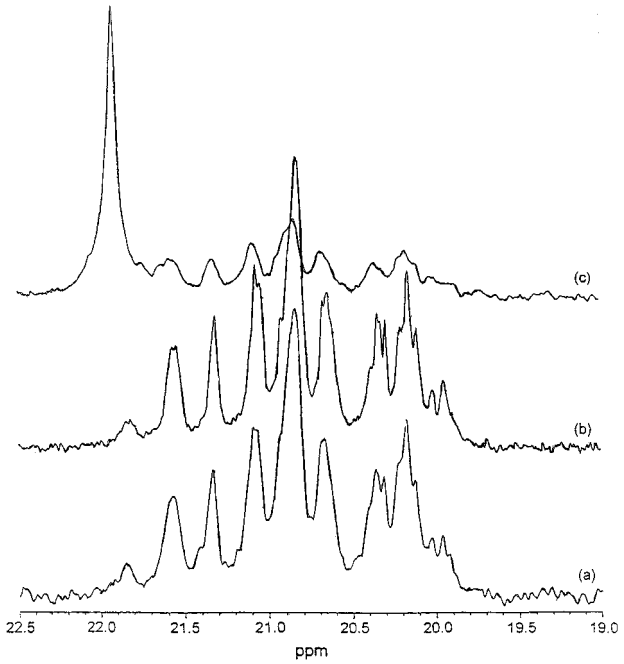

Figure 14. Methyl region of ^{13}C-NMR spectra of (a) *a*-PP (D55) and of D76 PP produced in the presence of **2**/**3** in a 2:8 ratio activated by **4**/TIBA for the (b) hexane-soluble fraction and (c) hexane-insoluble fraction.

Table 6. Solvent Fractionation of PP D52

				% stereoblock	
D52 solvent	% fraction	% [*mmmm*]	% other pentads	in fraction	in total polymer
acetone	< 0.1				0
ethyl ether	50.7	2.8	97.2	0	0
pentane	< 0.1				0
hexane	< 0.1				0
heptane	0.5	20.4	79.6	100	0.5
insoluble	48.6	89.3	10.7	13	6.5
tot.	100				7.0

0.5% stereoblock materials. Therefore, there is a total of about 7% stereoblock polymers in D52.

The finding of *sb*-PP among the products of single-site catalysis is unexpected even for *HBC systems* (*vide infra*). The stereorigid ligand framework of the *ansa*-zirconocene would preclude oscillation between *rac*-like and *meso*-like sites as proposed by Waymouth et al.[17] for nonbridged, sterically encumbered zirconocenes.

Possible Mechanisms of Formation of Stereoblock Polypropylene. It is interesting and useful for the stimulation of further research to speculate on possible mechanisms by which *sb*-PP is formed in the present investigation. One possibility is that a growing chain undergoes β-hydrogen transfer to eliminate an α-olefin molecule of a certain molecular weight from one type of catalytic site which then reinserts into a catalytic site of another type. This is said to take place in the case of Dow's INSITE technology.[29] Dow's "constrained geometry catalyst" has a sterically open active center which is particularly favorable for the insertion of oligo-α-olefin to form polyolefins with long chain branching. The precursors of this work are not known to incorporate oligo-α-olefins. In fact, precursor **4** specifically has little or no facility to polymerize olefins having four or more carbon atoms.[14]

We recall that the dominant mechanism of chain termination in the heterogeneous $TiCl_3$ type Ziegler–Natta catalyst is transfer to aluminum alkyls.[2,30] In contrast, with a metallocene catalyst, when used with a MAO cocatalyst, with metal alkyl chain transfer is superseded by the β-hydrogen elimination process of chain termination. In the present case, the metallocenium species are formed[10d–j] by alkylation of the zirconocene dichloride with trialkyl aluminum (R_3Al) followed by alkyde anion extraction by **4**. When R_3Al is present in excess, it can promote the exchange of polypropylene chains between the two kinds of active centers and R_3Al to result in the formation of *sb*-PP. Siedle et al.[31] had employed ^{13}C NMR to demonstrate the occurrence of exchange of methyl groups between $(CH_3)_3Al$ and $Cp_2Zr(CH_3)_2$, $[C_5(CH_3)_5]_2Zr(CH_3)_2$, $Ind_2Zr(CH_3)_2$, or $Me_2Si(C_5H_4)_2Zr$. The authors proposed the participation of zirconocenium species in this type of exchanges, especially when MAO is the alkylaluminum compound.

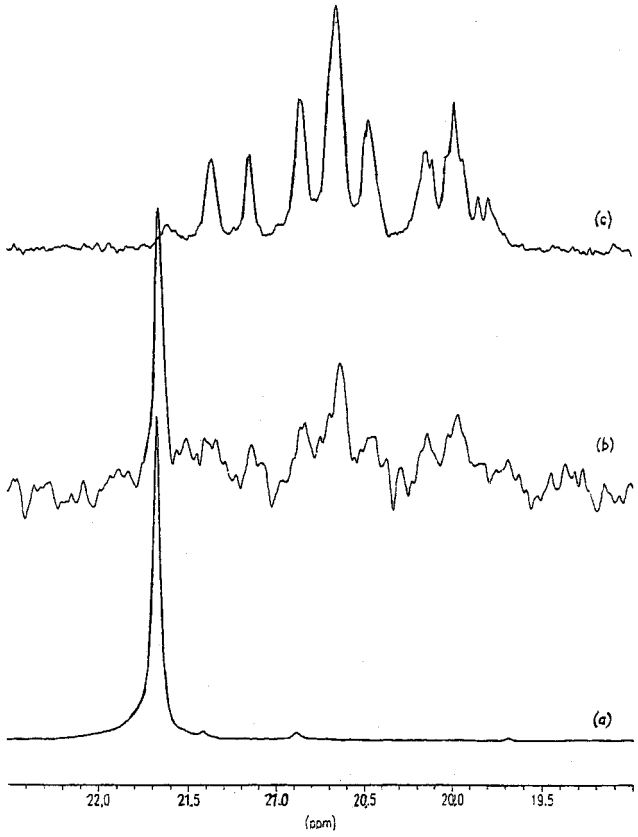

Figure 15. Methyl region of ^{13}C NMR of D52 PP produced in the presence of **2**/**3** in a 4:6 ratio activated by **4**/TIBA: (a) heptane-insoluble fraction, (b) heptane-soluble hexane insoluble fraction, and (c) diethyl ether soluble fraction.

Direct site-chain interchange between zirconocene species may also be important. An X-ray molecular structure had been determined for the catalytically active dimeric $[Cp''_2ZrMe(\mu\text{-}Me)MeZrCp''_2]^+[MePBB]^-$, where $Cp'' = \eta^5$-1,2-$Me_2C_5H_3$ and $MePBB = MeB(2C_6F_4\text{-}C_6F_5)_3$. The dimeric cation exhibits ethylene polymerization activity of *ca.* 7.8×10^6 g of polymer/((mol Zr^+) atm h) to produce polyethylene of $M_w = 4 \times 10^5$ and $M_w/M_n = 2.7$.[32] This is a model structure of an intermediate for site-chain exchange between a zirconocene alkyl and a zirconocenium alkyl species.

Radioactive isotopic labeling demonstrated that *ansa*-zirconocenes are nearly quantitatively converted to their active zirconocenium species by cocatalyst **4**/TIBA even at low temperature.[10e] Similar transformations occurred with non-bridged[33] and *ansa*-zirconocenes[10c] by MAO at ambient or higher temperatures. In such cases direct site-chain interchange may involve two zircono-

Table 7. Comparison of *el*-PP

el-PP type	% Elongation	% Tensile set	% Recovery	% *i*-PP	ref
B	300	82−93	69−73	∼60	6b
A	300	30−50	83−90	18	4
	300	50−120	60−83	39	
	300	100−200	33−60	93	
C	100		90		15,16
	200		86		
	300		81		
D	300	50	83		17
E	300		97		present work

cenium ions. The formation of an electron-deficient alkyl-bridged dimer may be facilitated by the two cationic centers, which is, however, opposed by Coulombic forces. The fact that the positive change is believed to be extensively delocalized may mitigate against the electrostatic repulsion to some degree. However, evidence for this type of intermediate is lacking.

Occurrence of site-chain exchange was suggested by the difference in the stereospecificity of propylene polymerization in the presence of the racemic mixture and the *S* enantiomer of the bis(*O*-acetyl-(*R*)-mandelate of (*S*)-ethylenebis[4,5,6,7-tetrahydro-η^5-indenyl]zirconium cation.[34] The former produce PP of low stereoregularity and T_m, especially at high [Zr] and/or high [TIBA]. The latter afforded under any conditions PP of high T_m and high isotacticity, which is insensitive to either [Zr] or [TIBA]. These differences in polymerization stereospecificity catalyzed by the *R*/*S* and the *S* active centers alone may be explained by site-chain interchanges. When both *R* and *S* conters are present, the interchange of chain bound to the opposite antipodes followed by insertion of monomer in its preferred prochiral face results in a steric inversion of chain configuration. On the other hand if only one enantiomer S is present, there is no inversion of configuration as the result of site-chain interchange.

Regardless of the mechanism of the process of the *sb*-PP formation and the detailed microstructure for it, the material should be effective compatibilizer for *i*-PP and *a*-PP homopolymers.

Conclusion

In a recent report[35] thermoplastic elastomer (TPE) is said to be the only segment of the overall rubber industry which is rapidly growing. The annual growth rate is 5.6%; TPE is capturing market traditionally held not only by other elastomers but by a number of thermoplastics too.

Several methods had been developed to prepare *el*-PP. It is interesting to compare their elastic properties to promote further improvement. The expression which can be used to convert different elastic properties is

$$\%\ \text{recovery} = \frac{\%\ \text{max elongation} - \%\ \text{tensile set}}{\%\ \text{max elongation}} \times 100\% \quad (6)$$

The results are summarized in Table 7.

The catalysts employed by Wilson and Job[6] are heterogeneous mixtures. They produce *el*-PP-**B**, which comprises isotactic, atactic, and syndiotactic sequences with high tensile set and poor recovery. The *el*-PP-**A** described by Collette et al.[5] and blends with *i*-PP are also poor in elasticity. Both *el*-PP-**C** and **D** are formed by site-switching catalysts.[15−17] They have about 80% recovery at 300% elongation. The block lengths are rather short in these *sb*-PP moieties.

The TPE-PP of this work exhibits excellent elastic recovery which is insensitive to elongation up to 500%. The strength of the material probably derives from the high molecular weight of the *a*-PP (500 000) and of the *i*-PP (180 000), bound together by *sb*-PP into highly branched (dendritic) superstructures.

The present *HBC* synthesis of *el*-PP is very versatile. By selecting the appropriate C_2 and C_{2v} symmetric metallocenes, elastic materials of desired molecular weights and stereoregularity can be produced which have desired phase transition temperature, Young's modulus, elastic recovery, and other properties. For a given C_2 symmetric stereorigid precursor, polymerization conditions such as T_p, [monomer], [H_2], [cocatalyst], and solvent polarity can be utilized to fine tune the structure and properties of the crystalline component, as had been detailed for **1**[10a] and **2**.[10e] Furthermore, similar influences on the structure of *a*-PP can be affected by experimental conditions as reported for **3**.[14,36] The combined effects of the conditions of polymerization can produce many types of naturally compatible blends of *i*-PP/*a*-PP as shown in Tables 1 and 2.

The principles described above have been extended to synthesize other naturally compatible blends such as *s*-PP/*a*-PP and *s*-PP/*i*-PP.[37]

Previously mixtures of titanocene and zirconocene[38] and of zirconocene and hafnocene[39] were employed with MAO cocatalyst to synthesize polyethylene having bimodal molecular weight distribution. GPC chromatograms of the product were faithful superpositions of similar polymerization using the two metallocenes separately. Neither the structure nor the properties of polyethylene would be noticeably affected by site-chain interchange except for a narrowing of molecular weight distribution as compared to the total absence of site-chain interchange for *HBC* polymerization.

Acknowledgment. Y.I. was on leave and supported by UBE Industries. The assistance of L. E. Dickinson on NMR, R. Farris on mechanical properties and MRSEC on XRD measurements is acknowledged.

References and Notes

(1) Natta, G. *J. Polym. Sci.* **1959**, *34*, 531.
(2) Natta, G.; Mazzanti, G.; Crespi, G.; Moraglio, G. *Chim. Ind. (Milan)* **1957**, *39*, 27.
(3) For monographs and symoposia volumes: (a) Boor, J. Jr. *Ziegler-Natta Catalysts and Polymerizations*; Academic: New York, 1979. (b) Chien, J. C. W. *Coordination Polymerization*; Academic: New York, 1975. (c) Lenz, R. W.; Ciardelli, F. *Preparation and Properties of Stereoregular Polymers*; D. Reidel Pub.: Dordrecht, The Netherlands, 1980. (d) Kissin, Y. V. *Isospecific Polymerization of Olefins*; Springer-Verlag: New York, 1985.
(4) (a) Kontos, E. G. U.S. Patent 3,378,606, April 16, 1968. (b) Kontos, E. G. U.S. Patent 3,853,969, Dec 10, 1974. (c) Gobran, R.; *et al.* U.S. Patent 3,784,502, Jan 8, 1974.
(5) (a) Collette, J. W.; Tullock, C. W. Patent GB 2,001,080, 1978. (b) Collette, J. W.; Tullock, C. W. U.S. Patent 4,335,225, June 15, 1982. (c) Collette, J. W.; Tullock, C. W.; MacDonald, R. N.; Buck, W. H.; Su, A. C. L.; Harrell, J. R.; Mülhaupt, R.; Anderson, B. C. *Macromolecules* **1989**, *22*, 3851. (d) Tullock, C. W.; Mülhaupt, R.; Ittel, S. D. *Makromol. Chem. Rapid Commun.* **1989**, *10*, 19. (e) Tullock, C. W.; Tebbe, F. N.; Mülhaupt, R.; Ovenall, D. W.; Setterquist, R. A.; Ittel, S. D. *J. Polym. Sci. Part A, Polym. Chem.* **1989**, *27*, 3063.
(6) (a) Wilson, S. E.; Job, R. C. U.S. Patent 4,971,936, Nov 20, 1990. (b) Job, R. C. U.S. Patent 5,270,410, Dec. 14, 1993.
(7) Job[6b] employed a variety of reagents to modify the reaction of $Mg(OC_2H_5)_2$ and $TiCl_4$ to form catalysts which produce *el*-

PP having predominently syndiotactic sequences and minor amounts of isotactic and atactic sequences.
(8) For recent reviews see: (a) Brintzinger, H. H.; Fischer, D.; Mülhaupt, R.; Rieger, B.; Waymouth, R. M. *Angew. Chem., Int. Ed. Engl.* **1995**, *34*, 1143. (b) Möhring, P. C.; Coville, N. J. *J. Organomet. Chem.* **1994**, *479*, 1. (c) Horton, A. D. *TPIP* **1994**, *2*, 158. (d) Gupta, V. K.; Satish, S.; Bhardwaj, *J. Macromol. Sci., Rev. Macromol. Chem. Phys.* **1994**, *C34*, 439.
(9) (a) Kaminsky, W.; Külper, K.; Brintzinger, H. H.; Wild, F. R. W. P. *Angew. Chem., Int. Ed. Engl.* **1985**, *24*, 307. (b) Ewen, J. A. *J. Am. Chem. Soc.* **1984**, *106*, 6355.
(10) (a) Rieger, B.; Chien, J. C. W. *Polym. Bull.* **1989**, *21*, 159. (b) Rieger, B.; Mu, X.; Mallin, D. T.; Rausch, M. D.; Chien, J. C. W. *Macromolecules* **1990**, *23*, 3559. (c) Chien, J. C. W.; Sugimoto, R. *J. Polym. Sci. Part A, Polym. Chem.* **1991**, *29*, 459. (d) Chien, J. C. W.; Tsai, W.-M.; Rausch, M. D. *J. Am. Chem. Soc.* **1991**, *113*, 8570. (e) Chien, J. C. W.; Tsai, W.-M. *Makromol. Chem. Macromol. Symp.* **1993**, *66*, 141. (f) Tsai, W.-M.; Rausch, M. D.; Chien, J. C. W. *Appl. Organomet. Chem.* **1993**, *7*, 71. (g) Tsai, W.-M.; Chien, J. C. W. *J. Polym. Sci. Part A, Polym. Chem.* **1994**, *32*, 149. (h) Chen, Y.-X.; Rausch, M. D.; Chien, J. C. W. *J. Organomet. Chem.* **1995**, *487*, 29. (i) Chen, Y.-X.; Rausch, M. D.; Chien, J. C. W. *Organometallics* **1994**, *13*, 748. (j) Chen, Y.-X.; Rausch, M. D.; Chien, J. C. W. *J. Polym. Sci. Part A, Polym. Chem.* **1995**, *33*, 2093.
(11) (a) Ewen, J. A.; Jones, R. L.; Razavi, A.; Ferrara, J. D. *J. Am. Chem. Soc.* **1988**, *110*, 6255. (b) Ewen, J. A.; Elder, M. J.; Jones, R. L.; Curtis, S.; Cheng, H. H. In *Catalytic Olefin Polymerization* Keii, T., Soga, K., Eds.; Elsevier, Kodansha: Tokyo, 1990; p 438. (c) Ewen, J. A.; Elder, M. J.; Jones, R. L.; Haspeslagh, L.; Atwood, J. L.; Bott, S. G.; Robinson, K. *Makromol. Chem. Macromol. Symp.* **1991**, *48/49*, 253.
(12) Fierro, R.; Yu, Z.; Rausch, M. D.; Dong, S. Alvarez, D.; Chien, J. C. W. *J. Polym. Sci. Part A, Polym. Chem.* **1994**, *32*, 661.
(13) (a) Alt, H. G.; Milims, W.; Balackal, S. J. *J. Organomet. Chem.* **1994**, *472*, 113. (b) Resconi, L.; Jones, R. L.; Albizzati, E.; Camurati, L.; Piemontesi, F.; Guglielmi, F.; Balbontin, G. *Polym. Prepr. (Am. Chem. Soc., Div. Polym. Chem.)* **1994**, *35*, 663. (c) Resconi, L.; Jones, R. L.; Rheingold, A. L.; Yap, G. P. A. *Organometallics* **1996**, *15*, 998.
(14) Chen, Y.-X.; Rausch, M. D.; Chien, J. C. W. *Macromolecules* **1995**, *28*, 5399.
(15) Chien, J. C. W.; Rausch, M. D. Patent GB 2,241,244B, July 6, 1994.
(16) (a) Mallin, D. T.; Rausch, M. D.; Lin, Y.-G.; Dong, S.-H.; Chien, J. C. W. *J. Am. Chem. Soc.* **1990**, *112*, 2030. (b) Lin, Y.-G.; Mallin, D. T.; Chien, J. C. W.; Winter, H. H. *Macromolecules* **1991**, *24*, 850. (c) Chien, J. C. W.; Rieger, B.; Sugimoto, R.; Mallin, D. T.; Rausch, M. D. In *Catalytic Olefin Polymerization*; Keii, T., Soga, K., Eds.; Kodansha: Tokyo, 1990; pp 535−574. (d) Llinas, G. H.; Dong, S.-H.; Mallin, D. T.; Rausch, M. D.; Lin, Y.-G.; Winter, H. H.; Chien, J. C. W. *Macromolecules* **1992**, *25*, 1242. (e) Chien, J. C. W.; Llinas, G. H.; Rausch, M. D.; Lin, Y.-G.; Winter, H. H.; Atwood, J. L.; Bott, S. G. *J. Am. Chem. Soc.* **1991**, *113*, 8569. (f) Chien, J. C. W.; Llinas, G. H.; Rausch, M. D.; Lin, Y.-G.; Winter, H. H.; Atwood, J. L.; Bott, S. G. *J. Polym. Sci. Part A, Polym. Chem.* **1990**, *30*, 2601. (g) Llinas, G. H.; Chien, J. C. W. *Polym. Bull.* **1992**, *28*, 41. (h) Cheng, H. H.; Babu, G. N.; Newmark, R. A.; Chien, J. C. W. *Macromolecules* **1992**, *25*, 6980. (i) Babu, G. N.; Newmark, R. A.; Cheng, H. N.; Llinas, G. H.; Chien, J. C. W. *Macromolecules* **1992**, *25*, 7400. (j) Llinas, G. H.; Day, R. O.; Rausch, M. D.; Chien, J. C. W. *Organometallics* **1993**, *12*, 1283.
(17) (a) Coates, G. W.; Waymouth, R. M. *Science* **1995**, *267*, 217. (b) Hauptman, E.; Waymouth, R. M. *J. Am. Chem. Soc.* **1995**, *117*, 11586.
(18) (a) Gauthier, W. J.; Corrigan, J. F.; Taylor, N. J.; Collins, S. *Macromolecules* **1995**, *28*, 3771. (b) Gauthier, W. J.; Collins, S. *Macromolecules* **1995**, *28*, 3779.
(19) Hermann, W. A.; Herdtweck, E. *Angew. Chem., Int. Ed. Engl.* **1989**, *28*, 1511.
(20) (a) Chien, J. C. W.; He, D. *J. Polym. Sci. Part A, Polym. Chem.* **1991**, *29*, 1603. (b) Chen, Y.-X.; Rausch, M. D.; Chien, J. C. W. *J. Polym. Sci. Part A, Polym. Chem.* **1995**, *33*, 2093.
(21) Chien, J. C. W. *J. Am. Chem. Soc.* **1971**, *93*, 4675.
(22) Pasquin, I. *Pure Appl. Chem.* **1967**, *15*, 465.
(23) Sacchi, M. C.; Zucchi, D.; Tritto, I.; Locatelli, P.; Dall'Occo, T. *Macromol. Rapid Commun.* **1995**, *16*, 581.
(24) Collins, S.; Kelly, W. M.; Holden, D. A. *Macromolecules* **1992**, *25*, 1780.
(25) Song, W.; Shackett, K.; Chien, J. C. W.; Rausch, M. D. *J. Organomet. Chem.* **1995**, *501*, 375.
(26) (a) Soga, K.; Kaminaka, M. *Makromol. Chem. Rapid Commun.* **1992**, *13*, 221. (b) Collins, S.; Kelly, W. M.; Holden, D. A. *Macromolecules* **1992**, *25*, 1780. (c) Kaminsky, W.; Renner, F. *Makromol. Chem., Rapid Commun.* **1993**, *14*, 239. (d) Soga, K.; Kim, H. J.; Shiono, T. *Makromol. Chem., Rapid Commun.* **1993**, *14*, 765. (e) Soga, K.; Kaminsky, M. *Makromol. Rapid Commun.* **1994**, *15*, 593.
(27) Kaminsky, W.; Renner, F.; Winkelbach, H. *Proc. Met. Con. '94* May 25−27, 1994, Houston, TX.
(28) Chambon, F.; Winter, H. H. *J. Rheol.* **1987**, *31*, 683.
(29) (a) Stevens, J. C.; et al. European Patent Application 416,-815 A2, Aug. 30, 1990. (b) Stevens, J. C. In *Catalyst Design for Tailor-Made Polyolefins*; Soga, K., Terano, M., Eds.; Kodansha: Tokyo 1994; pp 277−284.
(30) (a) Chien, J. C. W. *J. Polym. Sci. A* **1963**, *1*, 1839. (b) Chien, J. C. W.; Kuo, C. I. *J. Polym. Sci., Polym. Chem. Ed.* **1985**, *23*, 731. (c) Chien, J. C. W.; Kuo, C. I. *J. Polym. Sci., Polym. Chem. Ed.* **1986**, *24*, 1779.
(31) Siedle, A. R.; Newmark, R. A.; Lamanna, W. M.; Schwepper, J. N. *Polyhedron* **1990**, *9*, 301.
(32) Chen, Y.-X.; Stern, C. L.; Yang, S.; Marks, T. J. *J. Am. Chem. Soc.* **1996**, *118*, 12451.
(33) Chien, J. C. W.; Wang, B.-P. *J. Polym. Sci. Part A, Polym. Chem.* **1990**, *28*, 15.
(34) Song, W.; Yu, Z.-T.; Chien, J. C. W. *J. Organomet. Chem.* **1996**, *512*, 131.
(35) Reisch, M. S. *Chem. Eng. News.* **1996**, Aug 5, p 10.
(36) Resconi, L.; Jones, R. L.; Rheingold, A. L.; Yap, G. P. A. *Organometallics* **1996**, *15*, 998.
(37) Chien, J. C. W. To be submitted for publication.
(38) Ewen, J. A. In *Catalytic Polymerization of Olefins* Keii, T., Soga, K., Eds.; Studies in Surface Science and Catalysis 25; Kodansha: Tokyo, and Elsevier: Amsterdam, 1986; p 271.
(39) Ahlers, A.; Kaminsky, W. *Makromol. Chem. Rapid Commun.* **1988**, *9*, 457.

MA961726B